Surrogate Model for the Prediction of the Performance of a Tubular Pulsated Heat Pipe

Mouret Gaëlle[1], Becerril César[1], Ibrahim Mira[1], Cataldo Filippo[2]
[1]Capgemini Engineering
4 av. Didier Daurat, Blagnac, France
gaelle.mouret@capgemini.com; cesarantonio.becerrilaguirre@capgemini.com; mira.ibrahim@capgemini.com
[2]Wieland Provides
82 Via Piave, Latina, Italy
f.cataldo@provides.it

Abstract – Power electronics like Insulated Gate Bipolar Transistors (IGBT), Central Processing Units (CPU), Graphics Processing Units (GPU), and diodes, among others are key pieces for the control of electronics embedded in the new generation (more electrical) aircraft. These power electronics are smaller and more and more efficient. However, the increase in their performance and their miniaturization also increases their heat release. A solution to cool down these power electronics is the Pulsated Heat Pipes (PHP), which are very efficient and passive two-phase flow heat exchangers. This work discusses the construction of a PHP predesign tool using surrogate modelling. For this purpose, the database generation, surrogate training, and performance in predicting the thermal resistance of different PHP geometries are presented.

Keywords: thermal management, pulsated heat pipe, surrogate model, machine learning, Artificial Neural Network

1. Introduction

A Pulsating Heat Pipe [1] is a promising two-phase flow passive cooling technology that can be used to cool down the power electronics embedded in the new generation of aircraft. However, complex physical phenomena that occur within a PHP at a wide range of time and space scales make their performance difficult to predict. As a result, a lack of understanding and predictive tools for the design of PHPs prevents the deployment of this technology on an industrial scale.

To overcome this, the use of surrogate models trained with an experimental database and capable of predicting the performance of PHPs has been studied. Khandekar et al. [2] proposed an Artificial Neural Network predicting the thermal resistance from the filling ratio and the heat load. Lee and Chang [3] used NARX Neural Network to predict the evaporator temperature from the heat load. More recently, Jokar et al. [4] and Nerella et al. [5] used Artificial Neural Networks to predict the thermal resistance from its filling ratio, its heat load, and its inclination. All these studies showed good agreement between predictions and experiments. However, as their databases are built with a single prototype, they do not consider the geometrical parameters of the PHP. In addition, even if neural networks have proved their efficiency for the modelling of complex problems, other algorithms seem to be promising for building a surrogate model.

In this work, a broad database with different PHP geometries, low Global Warming Potential (GWP) refrigerants and multiple operating points is built. Then, this database is used to construct surrogate models capable of predicting the thermal resistance of a PHP from eleven geometrical and operational parameters. Six different algorithms are compared on their performance and accuracy. Then, the two best models are used to predict a new prototype.

2. Experimental Database

The database on which the model is trained has been thoroughly built. A Design of Experiment (DoE) using pseudo-random Halton sequences [6] was used to ensure that the design space was uniformly sampled. More information about the construction of the DoE can be found in [7]. The following paragraphs present the chosen parameters, ranges, and a brief overview of the obtained database.

2.1. Design of Experiment

Table 1 shows the input parameters of the mathematical model. They can be split into two categories: geometrical (lengths, diameter, U-turns) and operational (refrigerant, heat load, inclination,…). For design reasons the spacing between ducts is imposed: $E = 2*(D_{in} + 2e)$, where e is the wall thickness (unique for all prototypes), and the evaporator and condenser lengths are expressed as a percentage of the total length. The surface and total length of the prototypes can be computed from the other parameters.

Table 1: Parameters considered for the Design of Experiment and their ranges

Name	Geometrical					Operational					
	Total length	Cond. length	Evap. length	Nb. of Uturns	Inner diam.	Fluid	Filling ratio	Cold temp.	Pitch	Roll	Heat Load
Symbol	L_{tot}	L_{cond}	L_{evap}	Uturns	D_{in}	Fluid	FR	T_{cold}	α	β	Q
Units	m	%Ltot	%Ltot	-	mm	-	%	°C	°	°	W
Range	[0.15: 1.50]	[20:60]	[15:35]	[11:21]	[0.5:2]	R1233zdE R1234zeE R1234yf	[40:70]	[5:35]	[0:90]	[0:90]	rises until dry-out
Step	Cont.	Cont.	Cont.	2	0.5	-	15	15	45	45	

Drawing the geometrical and operational parameters leads to different prototypes for each experimental point. Although it would lead to an excellent database, it is not a realistic solution. Nine prototypes are thus drawn in a separate DoE and are presented in Table 2. For this geometrical DoE, a constraint is used on the evaporator and condenser surfaces to ensure they lay respectively between 130 and 780 cm² and 40 and 200 cm².

Table 2: Geometrical properties of the nine prototypes tested

Prototype	L_{tot} [m]	L_{cond} [m]	L_{evap} [m]	Uturns [-]	D_{in} [m]
1	0.186	0.058	0.019	19	0.002
2	0.282	0.164	0.035	21	0.002
3	1.245	0.410	0.067	13	0.001
4	0.818	0.222	0.072	15	0.001
5	0.445	0.227	0.054	17	0.0005
6	0.274	0.127	0.040	11	0.0015
7	0.489	0.248	0.049	17	0.0015
8	0.871	0.260	0.044	15	0.0015
9	1.445	0.303	0.077	11	0.0015

Then a second DoE is made from operational parameters for each prototype. The heat load is not considered in the DoE. For each point (i.e combination of prototype, fluid, FR, angles and cold source temperature) a series of measurements is done, starting with a heat load of 5W and increasing until dry-out or an evaporator temperature of 90°C is reached. A photograph of the experimental facility is shown on Fig. 2a. More details about the experiment can be found in [8].

2.2. Experimental database

The different prototypes tested worked unevenly. Some of them (prototypes 3 and 4, and prototype 5 to a lesser extent) had a bad thermal performance. The admissible power range was short and low, leading to a limited number of points, as illustrated on Fig. 2c). For these prototypes, the thermal resistance measured has a high median and an important standard deviation (Fig. 2b). For prototypes with a better performance, around one hundred points are registered (except for prototypes 1 and 2 that showed good performance and were widely explored). For these prototypes the thermal resistance is mainly below 1. The database totalizes 1098 points.
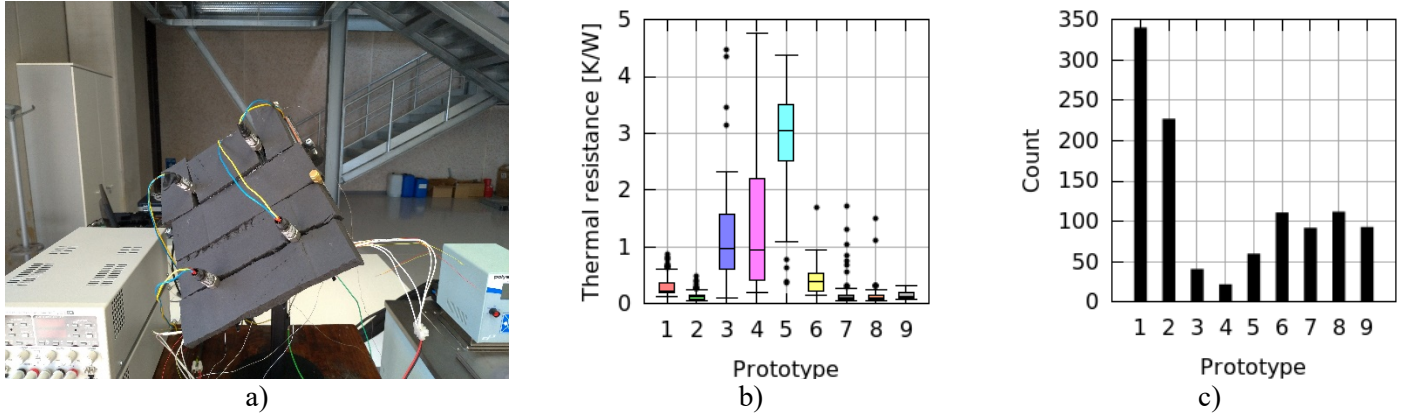
Fig. 1: a) Experimental facility b) Range of thermal resistance measured for each prototype and ~~b~~c) Count of points for each prototype

3. Presentation of the Surrogate Models

The construction of a surrogate model is basically based on the following method:

1. The model is trained over a percentage of a randomly chosen database (this subset of the database is called the training set). During this phase, the model parameters are adjusted to fit the data and minimize the error.
2. Then, the model is tested on the remaining part of the data (the testing set). If the prediction results are satisfactory (over the testing set), the process stops. If not, another iteration of training is performed. In the end, the user obtains a "transfer function". In this case, it will link the 11 inputs to the output (the thermal resistance).

To create the mathematical model, six different algorithms have been considered: Polynomial Regression (PR), Random Forest (RF), Artificial Neural Network (ANN), Polynomial Neural Network (PNN), Gaussian Process Regressor (GPR) and Kriging (KG). These methods have been implemented in a software named MAUS developed for the project, which has been successfully applied to several engineering problems.

The different methods are briefly presented in the following paragraphs. For each algorithm, one or more meta-parameters must be chosen. Obtained results are presented in part 4.

3.1. Polynomial regression (PR)

A polynomial function is used to fit as best the given data. The coefficients of the polynomial are adjusted to reduce an objective function of the form:

$$y_{estimate}(\beta_1, \dots, \beta_n) = \sum_i \left(y_{real,i} - \sum_j \beta_j x_j \right)^2 + \alpha \sum_j \beta_j^2 \qquad (1)$$

where the first term of this equation evaluates the training error, while the second term is a penalty function to limit the value of the found coefficients. The value of the polynomial coefficients and the penalty coefficient α are found using a Bayesian Ridge Regression [9].

3.2. Random Forests (RF) [10]

This method is an extension of the Decision Tree method, which allows building regression models in the form of a tree structure. The tree is composed of decision and leaf nodes. A condition is imposed on decision nodes and the result is given in the leaf nodes. The data is split into smaller subsets and the different subsets are grouped minimizing the mean squared error (MSE).

3.3. Gaussian Process Regression (GPR) [11]

Unlike the other regression algorithms that learn exact values for each parameter, GPR infers a probability distribution over all possible values. GPR is not limited by a functional form, so rather than calculating the probability function of a specific function, GPR calculates the probability distribution over all admissible functions that fit the data. However, the method specifies a prior Gaussian function, which is defined by a mean function and a covariance function named kernel. The key parameter of this method is the selection of its kernel, since it defines how similar f(xi) and f(xj) should be considering how similar xi and xj are.

3.4. Kriging (KG) [12]

This method is a particular case of GPR with a specific kernel (covariance function). Kriging postulates that the estimation at an unknown point (x_0) can be expressed as a linear combination of the output values at the other known points (x_i): $y_{estimate}(x_0) = \sum_i \lambda_i y(x_i)$. Therefore, this method can be reduced to searching the coefficients λ_i for each known point. These coefficients are chosen to minimize the variance error $E = (y_{estimate}(x) - y(x))^2$. In this case, the kernel is of the form: $C(x_i, x_j) = e^{-\theta|x_i - x_j|^{pl}}$ where parameters θ and pl are fitted during the training by a genetic algorithm or an optimiser.

3.5. Artificial Neural Networks (ANN)

There are different types of neural networks (NN). For this application, only Dense Feed Forward Neural Networks (DFFNN) [13] [14] are used. The NN is organized in layers composed of neurons. Each layer's neuron is linked to all the neurons of the next layer by weighted connections. To find the output of a neuron, the weighted sum (by the weights of their connections) of all the precedent neurons is computed and a bias term is added to this sum. This sum is passed through a (usually nonlinear) activation function to produce the output. The result of the neural network can be expressed as the matrix product of each layer. This surrogate requires the tuning of multiple parameters (number of neurons per layer, number of hidden layers, activation functions, and so on) to have an optimal result.

3.6. Polynomial Neural Networks (PNN) [15]

PNN is a neural network in which the activation function is the identity function, each neuron has two inputs, and its output is based on a reference function (linear, quadratic, cubic or linear covariance).

4. Application to full experimental database

The inputs of the models are the parameters sampled in the DoE, except for the heat load which is converted into a heat flux. The output is the thermal resistance of the PHP, computed from the evaporator average temperature measured at four different positions:

$$R_{th} = \frac{T_{evap} - T_{cond}}{Q}. \tag{2}$$

For each method, the meta-parameters are optimized over a wide range of values. Only the models with the best results are shown and re-used in section 4.2. The meta-parameters leading to these models are summarized in Table 3.

Table 3: Meta-parameters chosen for each method

PR	RF	PNN	GPR	ANN	KG
Order : 5	Max leaves: No Tree: 800	Function: quadratic	Kernel: Matern Nstarts: 150	Layers:4 Neurons:15 Optim: Nadam Acivation: softsign Learning rate : 0.004	Function: pso

4.1. Full database

For all the trainings, the data was split into a training set (80%) and a testing set (20%). The mean absolute and relative errors on the test set are plotted for each algorithm on Fig. 3. Random Forest and artificial neural network models provide the best results with a mean absolute error of 12% and 15%, respectively. Kriging is also an interesting candidate with an error of 19%. Polynomial regression, polynomial neural network and gaussian process regressor give the poorest results with an absolute error of 27%, 48% and 56%, respectively. PNN largely overestimates the thermal resistance, but there is no clear trend for the other methods for which the mean relative error remains between +/- 5%.
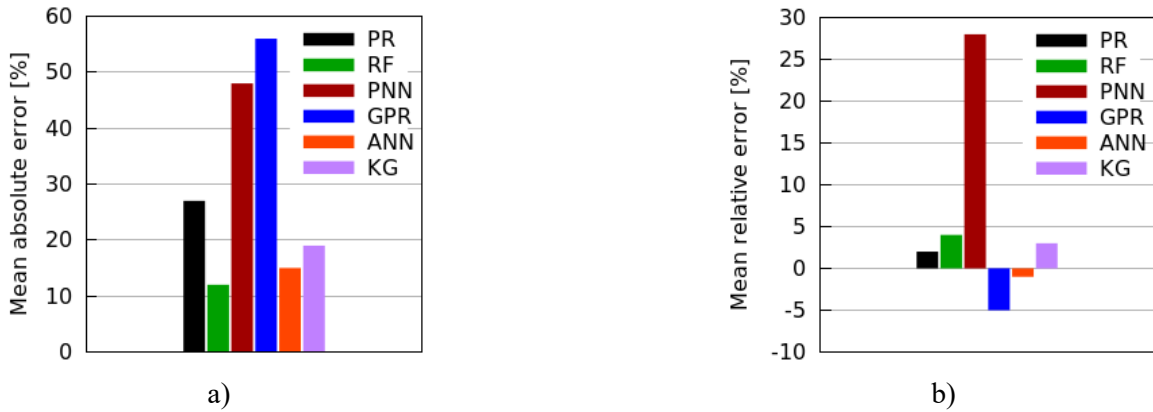

Fig. 2: a) Mean absolute error and b) Mean relative error obtained with the different methods trained with a 80/20 split of the database

Fig. 4a) plots the predicted thermal resistance obtained with the random forests model against the measured thermal resistance for all the prototypes. If the prediction was perfect, all the points would be on the f(x) = x line. Prototypes 1, 2 and 6 to 9 are well predicted. The error is mainly caused by prototypes 3 and 4 and to a lesser extent by prototype 5. Fig. 4b) shows that the error decreases when the heat load increases, even for prototypes with low thermal resistance like prototypes 1 and 2. At low heat load, the PHP is not completely started-up on its pulsating cycle, and once it is strong gradients of temperature and pressure appear and are responsible for the lack of accuracy of the models in this zone. It can be an important problem for the prediction of a new prototype functioning in this range. As the database cannot be refined to solve this problem, a solution could be to train different models by segregating the data on the heat load.
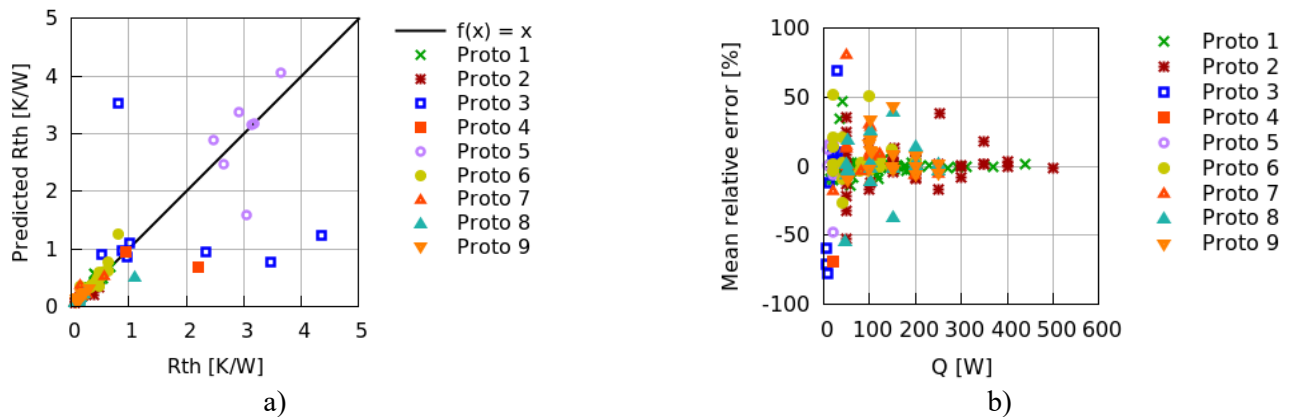

Fig. 3: a) Predicted thermal resistance versus measured thermal resistance and b) relative error versus heat load obtained with Random Forests for each prototype

4.2. Prediction of a new prototype

Random Forest and Artificial Neural Network models are now used to predict a new prototype, i.e., a prototype which is not used for the training of the model. Models are trained over 8 prototypes out of 9 (with a 90/10 split) and used to predict the remaining one. The meta-parameters used are the same as in section 4 (see Table 3).

For both ANN and RF, three models are trained using three different data sets: heat loads above 50W, heat loads below 50W, and all the heat loads. The objective is to determine if using nested models improves the prediction by avoiding the pollution of the whole domain by the area with strong gradients. The prediction of the new prototype is made twice for comparison: first with the model trained on the whole data (ALL) and second with the combination of the two models trained separately on low and high heat loads (SEP trained respectively on low Q and high Q).

This process is repeated for the prediction of three prototypes:
- Prototype 1 is the shortest one (L_{tot} = 0.186 m): an extrapolation is performed. The range of heat loads for this prototype is 5 to 500W.
- Prototype 3 is the second longest prototype (L_{tot} = 1.245 m) with poor performance. An extrapolation is performed. This prototype ranges only thermal loads below 50 W (between 5 and 40 W).
- Prototype 8 has medium geometrical characteristics: an interpolation is performed. Thermal loads are above 50 W (from 50 to 400W).

This leads to a total of 9 trained models. The mean absolute error is computed on the whole prediction (ALL on the x-axis) but also separately on low and high heat loads. For prototype 3(cf. Fig. 5b)), since all the heat loads are below 50W only the low Q and the ALL Q models were triggered. For prototype 8 (cf. Fig. 5c)), all the heat loads are above 50W, therefore only the high Q and ALL Q models were triggered. Results are presented on Fig. 5 respectively for prototypes 1 (a), 3 (b) and 8 (c).
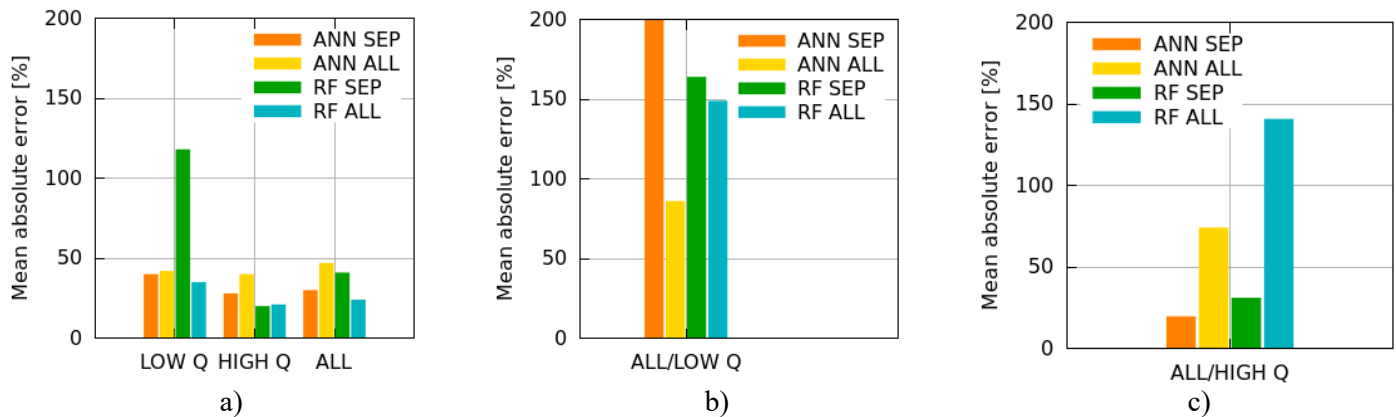

Fig. 4: Mean absolute error obtained with Artificial Neural Networks and Random Forests with separate or not models for the prediction of prototype 1 (a), prototype 3 (b) and prototype 8 (c)

Fig. 4a) and 4.b) show that, for the prediction of low heat loads, the accuracy decreases when separate models are used instead of a unique model. On prototype 1, the impact is neglectable with Neural Network models (-2 points) but the RF SEP fails to predict the thermal resistance, while the RF ALL shows the best result (35%). ANN ALL achieves the prediction of prototype 3 with the smallest error (86%).

On the opposite, using nested models improves the prediction of high heat loads. For example, on prototype 1 the error is decreased by 12 points with ANN SEP compared to ANN ALL and by 2 points with RF SEP compared to RF ALL. However, on prototype 8, it is decreased by 54 points with ANN SEP and an error of 31% is obtained with RF SEP while RF ALL failed to predict this prototype.

According to these results, a good solution would be to use two different models: a first one trained with heat loads above 50W and used to predict the same range of heat loads, and a second one trained with the whole dataset and used to to predict heat loads below 50W. Moreover, it is also interesting to evaluate the performance of the surrogate models not not only in predicting thermal resistance but also in predicting tendencies.

Therefore, the evolution of the thermal resistance with the heat flux is plotted for three series of experiments on Figure Figure 6. Figures a), b) and c) correspond respectively to prototypes1, 3 and 8. The corresponding conditions can be found in Table 4.

Figure 6a) illustrates that, if separate models give a lower error on the thermal resistance, they can predict badly the slope of the curve. In the frame of this project, as the objective is to minimise the absolute error, the best solution is to use two different models. However, it is up to the user to adjust his strategy depending on his objectives. Figure 6b) shows how the thermal resistance is overestimated in the case of prototype 3 due to the strong gradient in this domain. Using the whole dataset instead of only heat load below 50W helps the model to get the overall picture and better predict this prototype. On the opposite, it can be seen on Figure 6c) that the prediction of high heat loads is disturbed by considering the strong gradients of low heat loads. Only separate models succeed in capturing both the value and the slope of the thermal resistance.

Table 4: Conditions of the three experiments plotted in Figure 6

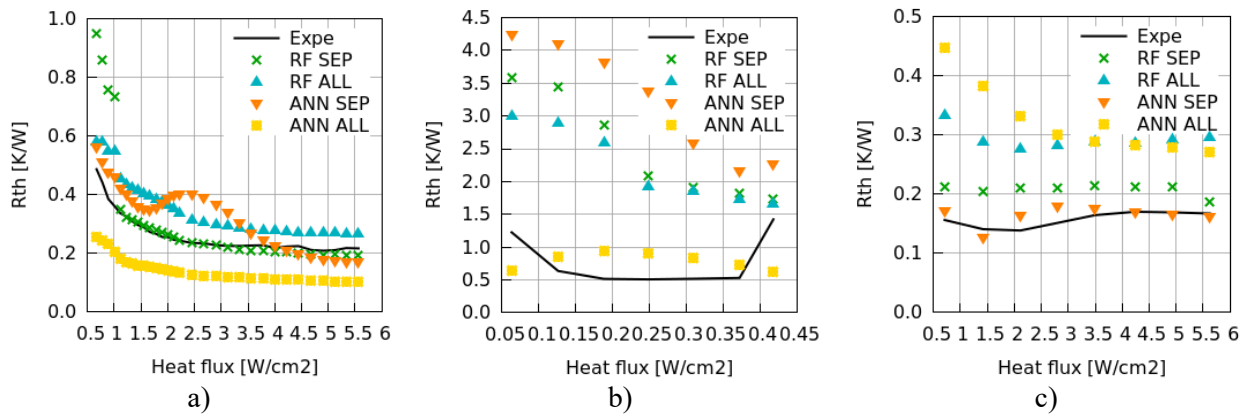| Figure	Prototype	Fluid	FR [%]	T_{cold} [°C]	Pitch [°]	Roll [°]
a)	1	R1233zdE	40	20	0	0
b)	3	R1233zdE	40	20	90	0
c)	8	R1234yf	70	35	90	0

Figure 5: Evolution of the thermal resistance with the heat flux for the experiment and the four models tested for prototypes-1 (a), 3 (b) and 8 (c).

5. Conclusion and further work

An experimental database is created based on a design of experiments. Eleven parameters are studied: five geometrical (total length, evaporator length, condenser length, number of U-turns and inner diameter) and six operational (fluid, filling ratio, cold source temperature, pitch, roll and heat flux). The database totalizes 1098 points and is used to train surrogate models. Six algorithms are used and compared: polynomial regression, random forests, artificial neural network, polynomial neural network, Gaussian process regressor and Kriging. When the model is trained over 80% of the dataset and tested over the 20% left (randomly split), random forests and artificial neural network models show the best results with a mean absolute error on the predicted thermal resistance below 15%. These two methods are then used to predict a new prototype, i.e., a prototype not used for the training. Using two models to predict low or high heat loads allows computing the new prototype

with an acceptable error (around 30%) for prototypes with a geometry close to the existing prototypes. The error on a more challenging prototype (i.e., with a very different geometry) is more important (around 80%).

These results could be improved by identifying the functioning mode (pulsating or conduction) of each point. This model can be extended to a wider range of applications by adding new experimental points to the database. The model can also be used to perform an extrapolation, but the accuracy cannot be guaranteed.

Acknowledgements

References

[1] H. Akachi, F. Polášek, and P. Štulc, "Pulsating Heat Pipes", *Proc. 5th Int. Heat Pipe Symp.*, Melbourne, Australia, pp. 208-217, 1996

[2] S. Khandekar, X. Cui, M. Groll, "Thermal performance modeling of pulsating heat pipes by artificial neural network", *Proceedings of 12th International Heat Pipe Conference*, pp. 215-219, 2002

[3] Y.W. Lee and T.L. Chang, "Application of NARX neural networks in thermal dynamics identification of a pulsating heat pipe", *Energy Convers Manag.*, vol. 50, pp. 1069–1078, 2009

[4] A. Jokar, A.A. Godarzi, M. Saber and M.B. Shafii, "Simulation and optimization of a pulsating heat pipe using artificial neural network and genetic algorithm", *Heat and Mass Transfer*, vol. 52(11), 2016

[5] S.S. Nerella, S.V.V.S. Nakka and B. Panitapu, "Mathematical modelling of closed loop pulsating heat pipe by using artificial neural networks", Int. J. Heat Technol., vol.39(3), pp. 955-962, 2021

[6] X. Wang and F. Hickernell, "Randomized Halton sequences", *Math. Comp. Model.*, vol. 32, pp887-899, 2000.

[7] C. Becerril, G. Mouret and F.M Mancio Reis, "Passive Light-Weight Cooling of Aircraft Electronics with Pulsating Heat Pipes, Part 3: A predesign surrogate model for tubular", *Proceedings of More Electric Aircraft Conference*, Bordeaux, France, 2021

[8] G. Rouaze, J.B. Marcinichen, F. Cataldo, P. Aubin and J.R. Thome, "Simulation and experimental validation of pulsating heat pipes", *Applied Thermal Engineering*, vol. 196, pp 1-11, 2021.

[9] D. MacKay, "Bayesian Interpolation", *Neural Comput.*, vol. 4, pp. 415- 447, 1991

[10] D. Steinberg and P. Colla, "CART: Classification And Regression Trees", in *The top ten algorithms in data mining*, 2009 p. 179.

[11] C. Rasmussen, "Gaussian Processes in machine learning", Summer school on machine learning, pp. 63-71, 2003.

[12] W. Press, S. Teukolsky, W. Vetterling and B. Flannery, "Interpolation by Kriging", *in Numerical Recipes: The Art of Scientific Computing*, Cambridge University Press, 2007.

[13] P. Tahmasebi and A. Hezarkhani, "Application of a Modular Feedforward Neural Network for Grade Estimation", *Natural Resources Research*, vol. 20, pp. 25-32, 2011.

[14] J. Schmidhuber, "Deep learning in neural networks: An overview", *Neural Networks*, vol. 61, pp. 85-117, 2015.

[15] S. Oh, W. Pedrycz and B. Park, "Polynomial neural networks architecture: analysis and design", *Computers & Electrical Engineering*, vol. 29, pp. 703- 725, 2003.